



Article

Genome-Wide Analyses Reveal the Roles of CCT Genes as Regulators of Abiotic Stress Responses in *Citrullus lanatus*

Yajie Hong^{1,3,†}, Mengsha Li^{1,†}, Wona Ding¹, Jun Shi^{2,4}, Zishuo Zheng¹, Nailin Xing^{2,4,*} and Qiuping Li^{1,*}

- ¹ Ningbo Key Laboratory of Agricultural Germplasm Resources Mining and Environmental Regulation, College of Science & Technology, Ningbo University, Ningbo 315300, China; 2311130014@nbu.edu.cn (Y.H.); limengsha@nbu.edu.cn (M.L.); dwn@zju.edu.cn (W.D.); zhengzishuo2@outlook.com (Z.Z.)
- ² Ningbo Key Laboratory of Characteristic Horticultural Crops in Quality Adjustment and Resistance Breeding, Ningbo 315040, China; shijunfred@163.com
- ³ Ningbo University, Ningbo 315211, China
- ⁴ Ningbo Academy of Agricultural Sciences, Ningbo 315040, China
- * Correspondence: xingnailin@hotmail.com (N.X.); liqiuping2@nbu.edu.cn (Q.L.); Tel.: +86-187-5741-6481 (Q.L.)
- † These authors contributed equally to this work.

Abstract: Members of the CCT gene family have been shown to play roles in photoperiodic flowering and environmental adaptation under a range of conditions. In this study, 29 CCT genes from watermelon were categorized into three distinct subfamilies. The CICCT genes were systematically analyzed, focusing on their physicochemical properties, gene duplication, motifs, structural divergence, promoter regions, and collinearity with genes from other species. The responsiveness of these genes to abiotic stressors, hormone treatments, and photoperiod prolongation was also examined. Segmental duplication (gene amplification) significantly influenced the evolution of these genes, with most CICCT genes containing light-, hormone-, and/or abiotic stimulus-responsive elements. In response to abiotic and hormonal stresses, 5 genes responded to cold, 1 gene to drought, and 4 genes to salt. 6 genes were responsive to ABA, and 13 genes to MeJA. Strikingly, *CICCT17*, *CICCT4*, and *CICCT28* responded to multiple stressors. A majority of these CICCT genes and their homologs in other species were responsive to prolonged daylight exposure. The varying expression patterns of these genes suggested a key role for watermelon CCT genes in the regulation of both abiotic stress responses and flowering. Functional diversity was also evident among CCT family genes within a given species as well as among species attributable to changes in the structural features and expression patterns of the genes and the encoded proteins.

Keywords: watermelon; CCT gene; abiotic stress; expression analysis



Academic Editors:
Salvatore Ceccarelli and Eleni Tani

Received: 16 December 2024
Revised: 5 January 2025
Accepted: 16 January 2025
Published: 18 January 2025

Citation: Hong, Y.; Li, M.; Ding, W.; Shi, J.; Zheng, Z.; Xing, N.; Li, Q.

Genome-Wide Analyses Reveal the Roles of CCT Genes as Regulators of Abiotic Stress Responses in *Citrullus lanatus*. *Agronomy* **2025**, *15*, 232. <https://doi.org/10.3390/agronomy15010232>

Copyright: © 2025 by the authors. Licensee MDPI, Basel, Switzerland. This article is an open access article distributed under the terms and conditions of the Creative Commons Attribution (CC BY) license (<https://creativecommons.org/licenses/by/4.0/>).

1. Introduction

CCT genes encode proteins harboring a CCT (CONSTANS, CONSTANS-LIKE, and TOC1) domain. In addition to shaping plant photoperiod responsivity, these genes are crucially tied to phytohormone signal transduction and abiotic stress responses [1–4]. The C-terminus of these CCT domain-containing proteins harbors a 43–45 amino acid nuclear localization sequence. The features of conserved N-terminal domains can be further used to classify CCT family members into the COL subfamily, with an N-terminus containing one or two B-box domains (zinc ion binding domains), the PRR subfamily, with an N-terminus containing a REC domain (receiver domain), and the CMF subfamily lacking any conserved N-terminal domains [2].

Many plant CCT family members shape the timing of flowering in plant species [1–4]. These CCT domain genes directly or indirectly control flowering time, participate in circadian clock regulation, and are key components of light signaling [1–4]. Of the 41 CCT genes identified in rice to date, 18 play a role in controlling the timing of flowering [2,4]. The rice gene *DTH2*, a member of the COL family, promotes early flowering by upregulating the florigen genes *Hda* and *RFT1* under long-day conditions [5]. Similar or distinct mechanisms have also been identified through which CCT genes in other plants, including *CcCCT23*, *PPD1*, *SbGhd7*, *Ppd-H1*, *TaFT2*, *BvBBX19*, and *GmCOL1a*, which also regulate flowering timing [6–12]. Most CCT family genes (*COL1*, *COL2*, and *COL3*) are regulated by *COP1* and interact with downstream genes *FT* and *SOC1*, playing a role in the flowering process in *Arabidopsis thaliana* [13]. Certain CCT genes can extend the heading stage and thereby increase plant yields [1]. The rice gene *Ghd7*, containing a single CCT domain, represses the expression of *Ehd1* and *Hd3a* under long-day conditions, thus inhibiting reproductive development affecting heading date, plant height, and yield [14]. The sorghum *SbHd1* gene, as well as the rice *Hd1* and *Ghd7.1* genes, can all improve grain number through their effects on flowering time [1,15,16]. In *Arabidopsis*, *CO* can suppress *AP2* expression under short or long daylight conditions, thereby influencing seed size [17,18].

Abiotic stresses inhibit plant growth by reducing photosynthesis and altering the composition of bioactive compounds, ultimately impacting crop yield and quality [19–21]. Members of the CCT family of genes can also shape plant responses to abiotic stressors [22–25]. For example, *Ghd2* directly targets the promoter of *RCA*, upregulating its expression and increasing drought sensitivity [22]. *OsPRR73*, a member of the PRR gene subfamily, negatively regulates *OsHKT2;1*, reducing sodium influx and ROS accumulation, thereby conferring salt tolerance in rice [23]. The *AtCOL4* gene is capable of enhancing the tolerance of *Arabidopsis thaliana* to salt stress and functions through ABA-dependent signaling pathways [24]. Overexpressing *ZmCCT* can suppress *ZmVOZ1* and *ZmARR16* expression, leading to improved maize drought resistance under conditions of pro-longed daylight [25]. Many natural CCT family gene variants have been identified to date, and studies of these genes have the potential to aid efforts to develop improved crop varieties more adaptive to the conditions found in different regions [1].

Watermelons (*Citrullus lanatus*) are widely popular for their sweet and refreshing fruit and are cultivated globally for consumption. China leads the world in both watermelon production and cultivation area. The yield and quality of watermelons are influenced by various factors, including biotic stresses such as microorganisms and pests, as well as abiotic stresses like extreme temperatures, salt stress, and drought [19]. However, no systematic analyses of the watermelon CCT gene family, particularly regarding abiotic stresses, have been conducted to date. In this study, watermelon CCT genes were analyzed with a focus on their physicochemical features, gene duplication relationships, homology, and collinearity with those of other species. Moreover, the changing expression patterns of these genes in response to abiotic stressors, hormone stress, and prolonged daylight exposure were also examined. These analyses may identify genes involved in regulating abiotic stress responses and those responsive to long-day lengths, providing a foundation for improving watermelon varieties and offering insights for enhancing other crops in the future.

2. Materials and Methods

2.1. Experimental Material and Growth Conditions

Watermelon (*C. lanatus* L. cv. 8424) plants, which are sensitive to chilling, were used for cold treatment. Watermelon (*C. lanatus* L. cv. 97,103) plants, known for their strong adaptability, can be cultivated across a wide geographical range, from the south to the north, with rapid growth. The reference genome map of the watermelon cultivar 97,103 has

been published. Watermelon plants (*C. lanatus* L. cv. 97103) were used as phytohormones and treatments for long-day conditions. Watermelon (*C. lanatus* L. cv. 8424) seeds and watermelon (*C. lanatus* L. cv. 97,103) seeds were sown in 96-well plug trayse in a growth chamber (Yanghui Instrument Co. Ltd., Ningbo, China) with 28 °C/22 °C (16 h/8 h) day/night temperatures and a relative humidity of 75% [26].

The commercial watermelon cultivar Crimson Sweet, known for its high fruit yield and good quality, was used for salt and drought treatments. Crimson Sweet seeds were sown in 96-well plug trayse with soilless media and placed in a greenhouse with 30 ± 5 °C (16 h/8 h) day/night temperatures and relative humidity of 75% [27,28].

2.2. Stress Treatments

For phytohormone treatments, 4-week-old seedlings (*C. lanatus* L. cv. 97103) were sprayed with 100 µM of ABA (Sigma Chemical Co., St. Louis, MO, USA) or MeJA (Sigma Chemical Co., St. Louis, MO, USA) on their leaves for 12 h, while control seedlings were sprayed with purified water.

Transcriptomic sequencing data were also used to assess leaf responses to salt stress (GEO: GSE146087). Six-week-old Crimson Sweet seedlings, with three fully expanded leaves, were transferred to 50 mL centrifuge tubes containing 300 mmol NaCl (Sinopharm Chemical Reagent Co. Ltd., Shanghai, China), with purified water as the control. After 7 h of salt stress exposure, leaf tissue samples were collected from four independent seedlings and rapidly frozen in liquid nitrogen for further processing and storage at −80 °C [27].

Drought stress data (GEO: GSE144814) were obtained from the GEO database (<https://www.ncbi.nlm.nih.gov/gds/>) based on established CICCT identities. Eight-week-old Crimson Sweet seedlings were transplanted into round nursery pots filled with equal weight (~22 lb) of soil-less media, Absorb-N-Dry (Balcones Minerals Corporation, Flatonia, TX, USA), under the same conditions. The control group received regular irrigation to maintain a relative moisture content of 95 ± 5%. In contrast, for drought stress treatment, potted plants were subjected to drought by withholding water for 8 days after transplantation. Leaf tissue samples were collected from four independent seedlings and rapidly frozen in liquid nitrogen for further processing and storage at −80 °C [28].

Transcriptomic sequencing data corresponding to leaf responses to cold stress were also obtained from prior studies [26]. Fifteen-day-old seedlings of watermelon cultivar 8424 were transferred to growth chambers set at 24 °C or a freezing condition at −6 °C. After 2 days of treatment, leaves were collected from each plant.

As watermelon is a long-day plant, flowering is promoted when sunlight exceeds a specific threshold (i.e., critical sunshine length). The CICCT gene responses to prolonged daylight exposure were assessed by growing seedlings for 28 days under a 16/8 h light/dark regime at 25 °C. Every 4 h for a total of 24 h, the second-to-last leaves from three individual plants were collected for analysis.

The legend represents the logarithmic normalized FPKM. The log₂-transformed FPKM values were used to create a heatmap depicting the expression of each CICCT gene. The heatmap of the expression patterns of CCT genes was generated by TBtools v1.0 software.

2.3. qPCR

A Plant Tissue RNA Extraction Kit (Sangon Biotech, Shanghai, China) was used to extract total RNA, after which the HiScript II 1st Strand cDNA Synthesis Kit (Sangon Biotech, Shanghai, China) was used for cDNA preparation. A LightCycler[®] 96 instrument (Roche, Mannheim, Germany) and ChamQ Universal SYBR qPCR Master Mix (Vazyme, Nanjing, China) were used for qPCR analyses, with *Clactin* (gene ID: Cla007792) serving as a normalization control. Each reaction needs three technical replicates. Primer 5 was

used to design all primers (Table S1). Relative target gene expression was computed with the $2^{-\Delta\Delta C_t}$ method and statistically analyzed by *t*-tests.

2.4. CICCT Gene Identification, Characterization, and Chromosomal Localization

Watermelon reference genome, protein sequence, and related annotation files were accessed through the Cucurbit Genomics Database on 23 March 2022 (<http://www.cucurbitgenomics.org/>). The conserved domains present in watermelon CCT proteins were screened with the Pfam (PF06203) (<http://pfam.xfam.org/>), HMMER v2.0, and NCBI-CDD tools (<https://www.ncbi.nlm.nih.gov/cdd/>) on 23 March 2022. A Perl script was used in HMMER to assess the molecular weight, isoelectric point, and amino acid length values for identified watermelon CCT proteins [29]. The putative subcellular localization of the proteins encoded by identified CICCT genes was assessed with the Cell-PLoc Prediction system (<http://www.csbio.sjtu.edu.cn/bioinf/Cell-PLoc-2/>) and WoLF PSORT Prediction (<https://wolfpsort.hgc.jp/>) on 27 March 2022. The annotations associated with the watermelon CCT gene in the Cucurbit Genomics Database were used to establish the gene locations and chromosomal length-related information for these genes with the MapChart v2.32 software [30].

2.5. Collinearity Analyses of CICCT Genes

Collinearity analysis is highly significant in ecology and evolutionary biology, as it reveals genetic correlations among different species. Collinearity between CCT genes from *C. lanatus* and those of *A. thaliana*, *O. sativa*, and *L. siceraria* were analyzed with MCScanX, visualizing the results with Circos. Ks (synonymous substitutions), Ka (nonsynonymous substitutions), and the Ka/Ks ratio for each pair of duplicate CCT genes were established with the KaKs_Calculator 2.0 [31].

2.6. Phylogenetic Analyses

The CCT proteins of *C. lanatus*, *O. sativa*, *Arabidopsis*, *Lsiceraria*, and *Zea mays L* were accessed using the Cucurbit Genomics Database (<http://www.cucurbitgenomics.org/>) and the Ensemble Plants Database (<https://plants.ensembl.org/index.html>) on 23 March 2022. These CCT proteins were then subjected to phylogenetic analyses performed with ClustalW, constructing a neighbor-joining (NJ) phylogenetic tree in MEGA 7.0 with 1000 bootstrap replicates. The phylogenetic tree was viewed and annotated using the TBtools v1.0.

2.7. Conserved Motif, Gene Structure, and Cis-Acting Element Analyses

CCT gene family structural diversity was assessed in *C. lanatus* through amino acid sequence analyses of the encoded proteins performed with MEME (<http://meme-suite.org>) on 13 April 2022. Conserved domain analysis was conducted using MEME (<http://meme-suite.org>) on 13 April 2022, with the number of motifs set at 15 and motif widths ranging from 6 to 50 amino acids. TBtools v1.0 was used for the visualization of phylogenetic trees, conserved domains, and gene structures. The 1500 bp regions upstream of each CICCT gene were obtained from the genomic sequence for *C. lanatus* and analyzed with the PlantCARE database (<http://bioinformatics.psb.ugent.be/webtools/plantcare/html/>) on 18 April 2022 to identify cis-acting regulatory elements. GSDS 2.0 was used to visualize the results.

3. Results

3.1. CCT Gene Identification and Collinearity Analysis in *Citrullus Lanatus*

HMM searches and domain analyses identified a total of 29 predicted CCT genes in *Citrullus lanatus*, as well as 40 in *Arabidopsis*, 26 in *Lagenaria siceraria*, and 51 in maize

(Tables 1 and S2). These 29 putative CCT genes were designated *CICCT1-CICCT29* according to their chromosomal locations as determined using the Cucurbit Genomics Database. These *CICCT* proteins ranged in size from 18.7 kDa (*CICCT09*) to 124.6 kDa (*CICCT12*) and exhibited isoelectric points from 4.02 (*CICCT15*) to 10.13 (*CICCT28*) (Table 1). Sequence analyses indicated that these *CICCT* proteins were between 158 amino acids (*CICCT09*) and 1115 amino acids (*CICCT12*) long. Predictive analyses of their subcellular localization suggested that 22, 5, and 2 *CICCT* proteins, respectively, localize to the nucleus, chloroplasts, and cytosol (Table 1). CCT family members may thus play distinct functional roles in these different intracellular compartments.

Table 1. The information of CCT family members identified from *Citrullus lanatus* genome.

Gene Name	Gene ID	PL (aa)	MW (kDa)	Pi	SCLpred
<i>CICCT01</i>	Cl97C01G000070	701	77.6	7.22	nucl
<i>CICCT02</i>	Cl97C01G000500	282	32.0	5.13	nucl
<i>CICCT03</i>	Cl97C01G002570	330	37.1	5.25	nucl
<i>CICCT04</i>	Cl97C02G029560	407	44.4	5.19	nucl
<i>CICCT05</i>	Cl97C02G035020	409	45.2	6.38	nucl
<i>CICCT06</i>	Cl97C02G036700	417	45.5	5.01	nucl
<i>CICCT07</i>	Cl97C02G044440	263	30.4	6.25	nucl
<i>CICCT08</i>	Cl97C02G046550	163	19.6	9.46	chlo
<i>CICCT09</i>	Cl97C03G051160	158	18.7	9.07	nucl
<i>CICCT10</i>	Cl97C03G052770	257	28.4	7.01	nucl
<i>CICCT11</i>	Cl97C04G075410	779	85.2	8.01	chlo
<i>CICCT12</i>	Cl97C04G079000	1115	124.6	6.99	chlo
<i>CICCT13</i>	Cl97C05G091170	286	32.4	4.61	cyto
<i>CICCT14</i>	Cl97C05G104580	400	44.9	5.44	nucl
<i>CICCT15</i>	Cl97C06G117020	415	45.2	4.02	nucl
<i>CICCT16</i>	Cl97C06G122380	375	40.9	6.13	chlo
<i>CICCT17</i>	Cl97C06G124360	366	42.6	4.94	nucl
<i>CICCT18</i>	Cl97C07G142260	492	54.8	5.99	nucl
<i>CICCT19</i>	Cl97C07G143190	356	40.4	5.03	nucl
<i>CICCT20</i>	Cl97C08G148200	353	40.1	7.62	nucl
<i>CICCT21</i>	Cl97C08G154610	358	38.9	4.73	nucl
<i>CICCT22</i>	Cl97C08G154620	296	32.0	6.76	nucl
<i>CICCT23</i>	Cl97C08G157330	337	37.0	6.31	cyto
<i>CICCT24</i>	Cl97C09G163710	303	33.9	6.88	nucl
<i>CICCT25</i>	Cl97C09G177940	307	33.0	4.63	nucl
<i>CICCT26</i>	Cl97C09G180960	283	32.7	8.59	nucl
<i>CICCT27</i>	Cl97C09G184140	261	30.1	6.58	nucl
<i>CICCT28</i>	Cl97C11G217740	422	47.1	10.13	nucl
<i>CICCT29</i>	Cl97C11G218170	321	35.6	7.46	chlo

These 29 *CICCT* genes were found to be distributed across the 10 chromosomes of *Citrullus lanatus*, with none being present on chromosome 10 (Figure S1). In contrast,

five CICCT genes were encoded on chromosome 2, while four were encoded on each of chromosomes 8 and 9. Additionally, chromosomes 1 and 6 each encoded three CICCT genes, whereas two were present on chromosomes 3, 4, 5, and 11. Tandem duplication and segmental duplication events frequently shape gene family evolution and expansion. Only a single tandem duplication cluster (*CICCT21* and *CICCT22*) was evident on the same region of chromosome 8 as a pair of tandem repeat genes (Figure S1). Five pairs of duplicated segments (*CICCT02/CICCT13*, *CICCT08/CICCT10*, *CICCT14/CICCT17*, *CICCT14/CICCT20*, and *CICCT07/CICCT27*) were also observed (Figure 1). Segmental duplication events thus appear to be more important than tandem duplication events for the expansion of the watermelon CICCT gene family. Selection pressure for these segmental gene pairs was assessed based on the Ka/Ks ratios, revealing that these ratio values were less than 1 for each of these pairs, such that these CICCT genes may primarily have been located under purifying selection. The Ka/Ks values for *CICCT21/CICCT22* were also greater than 1, suggesting their evolution having taken place primarily via positive selection. The divergence times of these genes were also estimated, with Ks values for these CICCT genes ranging from 0.58 to 1.24 (~19.35 to 41.41 Myr) (Table S3). Genomic synteny between the CCT genes of different species, including *Citrullus lanatus*, *A. thaliana* (dicot), *O. sativa* (monocot), *Zea mays* L. (monocot), and *Lsiceraria* (dicot) were also conducted to better elucidate their evolutionary relationships. Only a single syntenic gene pair was observed between *Citrullus lanatus* (dicot) and *A. thaliana* (dicot), as compared to 27 between *Citrullus lanatus* and *Lsiceraria* (dicot) (Table S4 and Figure S2), 2 between *Citrullus lanatus* (dicot) and *Zea mays* L. (monocot), none between *Citrullus lanatus* (dicot) and *O. sativa* (monocot) (Table S4 and Figure S3), 33 between *O. sativa* (monocot) and *Zea mays* L. (monocot), and 1 between *O. sativa* (monocot) and *Zea mays* L. (monocot) (Table S4 and Figure S4). Of these orthologous pairs, *CICCT15* exhibited orthologs in *A. thaliana*, *Zea mays* L., and *Lsiceraria*, suggesting that it may have played key roles in the growth and evolution of these plants.

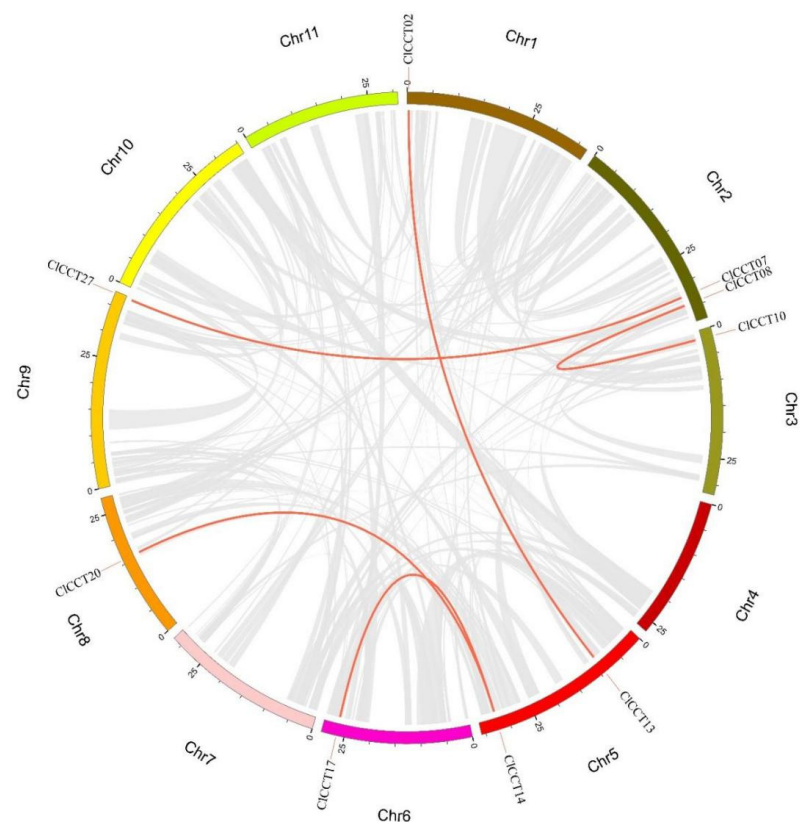


Figure 1. Collinearity analysis of CICCT genes. Red lines: segmentally duplicated gene pairs; gray lines: connect syntenic blocks in the genome.

3.2. Gene Structure, Conserved Motif, and Conserved Domain Analyses of CICCTs

CICCT protein sequence alignment results revealed a high degree of conservation among these various proteins in *Citrullus lanatus*. Figure S5 presents the logos and locations of these CICCT protein domains. The phylogenetic relationships among these CICCT members and their potential functional divergence were next explored, revealing the successful classification of these members into 8 groups in a phylogenetic tree constructed based on the protein sequences for the 29 CCT domains from these CICCTs (Figure 2A). To better characterize CICCT gene family conservation and diversification, the conserved protein motifs encoded by these genes and their associated exon-intron structures were analyzed. In total, 29 CICCT protein sequences were used to conduct conserved domain analyses (Figures 2B,C and 3). This led to the identification of 10 conserved motifs, with nearly identical conserved motifs within each of these subgroups. Those subgroups within the same group likely share conserved domains and may, therefore, function similarly (Figure 2B). The identified motifs were designated motif 1-motif 10 (Figure S6). Analyses of their sequences revealed that motif 4 was associated with more sequences than the other nine motifs. Motif 1 was present in all CICCT family members, and protein alignment logos indicated that motif 1 was associated with the CCT domain, demonstrating the high level of evolutionary conservation of this domain (Figures S5B and S6). Indeed, all CICCT proteins were found to harbor conserved CCT domains. In addition, 11 of these CICCT proteins were additionally found to harbor BBOX domains such that they were classified in the COL subfamily, while 3 harbored both CCT and REC domains such that they were classified in the PRR subfamily. Moreover, 15 CICCT family members harboring only a CCT domain were classified into the CMF subfamily. Of these CICCT proteins, four in the CMF subfamily (*CICCT21*, *22*, *24*, and *25*) also contained the GATA and TIFY domains (Figure S7). Notably, motifs 3 and 6 were only present among members of Group VIII in the CMF subfamily containing TIFY and GATA domains. Motif 4 was only present in Group VII proteins belonging to the PRR subfamily, suggesting that this motif may correspond to the REC domain. These factors may be relevant to the functional divergence of CCT family genes. Motif 2 was present in all members of Groups I, II, and IV belonging to the COL subfamily, suggesting that it corresponds to a component of the BBOX domain. Motifs 9 and 10 were respectively only observed in Groups I and II (Figures 2B and S7). Groups I, II, and IV may thus exhibit some degree of functional overlap while also exhibiting some degree of functional diversity. These motifs can, therefore, be used for the effective identification of different CICCT gene subsets that have undergone internal differentiation throughout evolution, potentially culminating in functional differentiation.

Structural analyses of these 29 CICCT genes revealed considerable variability in terms of their lengths and structural features. *CICCT21* was found to harbor 9 introns, whereas all identified members of groups II and IV exhibited a single intron and relatively simple, similar structures. All other members of the CICCT family harbored 2–9 introns, with most exhibiting consistent configurations in terms of their introns and exons within each subgroup, suggesting the greater conservation of genes within the same subgroups such that they may play similar biological roles (Figure 2C).

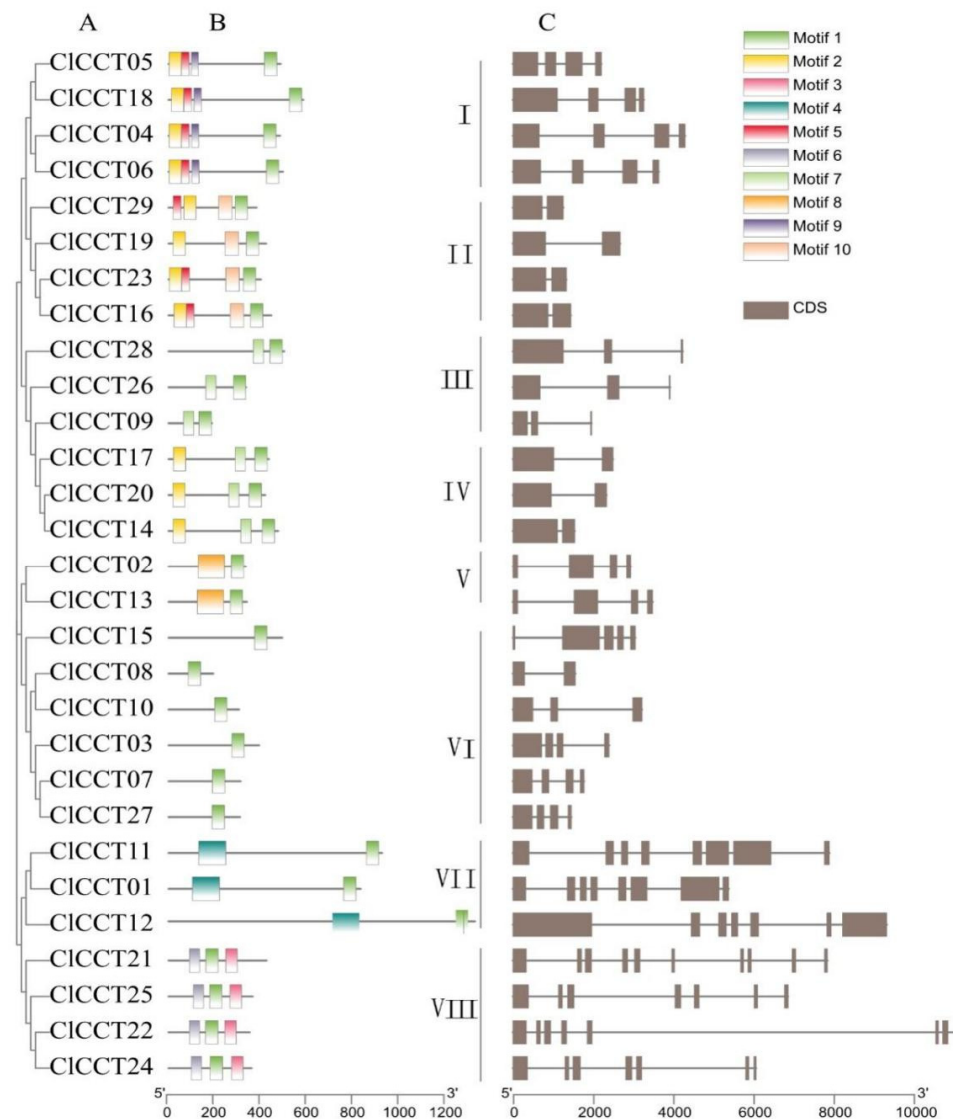


Figure 2. Phylogenetic relationship, motifs, and gene structures of the CICCT genes. (A) Phylogenetic tree. (B) Conserved motif. The colored boxes on the right denote 10 motifs. (C) Gene structure. The brown boxes and black lines represent exon and intron, respectively. The Roman numerals (I–VIII) indicate the structural groups.

3.3. Phylogenetic Analyses of Plant CCT Proteins

To explore the evolutionary relationships between watermelon CCT family members and those of other representative plant species, a neighbor-joining phylogenetic tree was constructed based on CCT-domain sequences. This tree incorporated 29 sequences from *Citrullus lanatus* (dicot), 40 from *Arabidopsis* (dicot), 26 from *Lagenaria siceraria* (dicot), 51 from maize (monocot), and 39 from rice (monocot) (Figure 3). The structures of these proteins were also established based on their conserved domains (Table S1), revealing the clustering of these 185 CCT proteins into four groups (A–D). All four groups were represented across all five species, with no branches being uniquely associated with any particular species, consistent with similar evolutionary patterns across species. Group A included 15 and 20 CCT proteins, respectively, belonging to the CMF and COL subfamilies, whereas Group C included 5 and 25 CCT proteins belonging to the CMF and COL subfamilies. Group B included 24 CCT proteins, among which the majority were members of the COL subfamily, while 5 and 2 were, respectively, members of the CMF and PRR subfamilies. Group D included 62 CCT proteins across these five species that were members of the CMF subfamily,

as well as 23 that were members of the PRR subfamily, except two *AtCCT* (*AT2G24790*), (*AT5G24930*) and one *OsCCT* (*OsCCT19*) that were COL subfamily members (Figure 3). These results indicated that CCT proteins emerged prior to the evolutionary divergence of monocots and dicots, with orthologous protein diversification among these plant species likely occurring following this split. Members of the CMF subfamily may have evolved from the COL subfamily via the degradation of the BBOX domains. Moreover, the CICCT genes were found to be highly homologous with those of *Arabidopsis thaliana*, bottle gourd, maize, and rice, consistent with high levels of conservation of these genes across species. The highest homology was evident when comparing these gene families in watermelons and bottle gourds. The similar protein sequences of these CCT family members suggest that they may play similar functional roles across these five species.

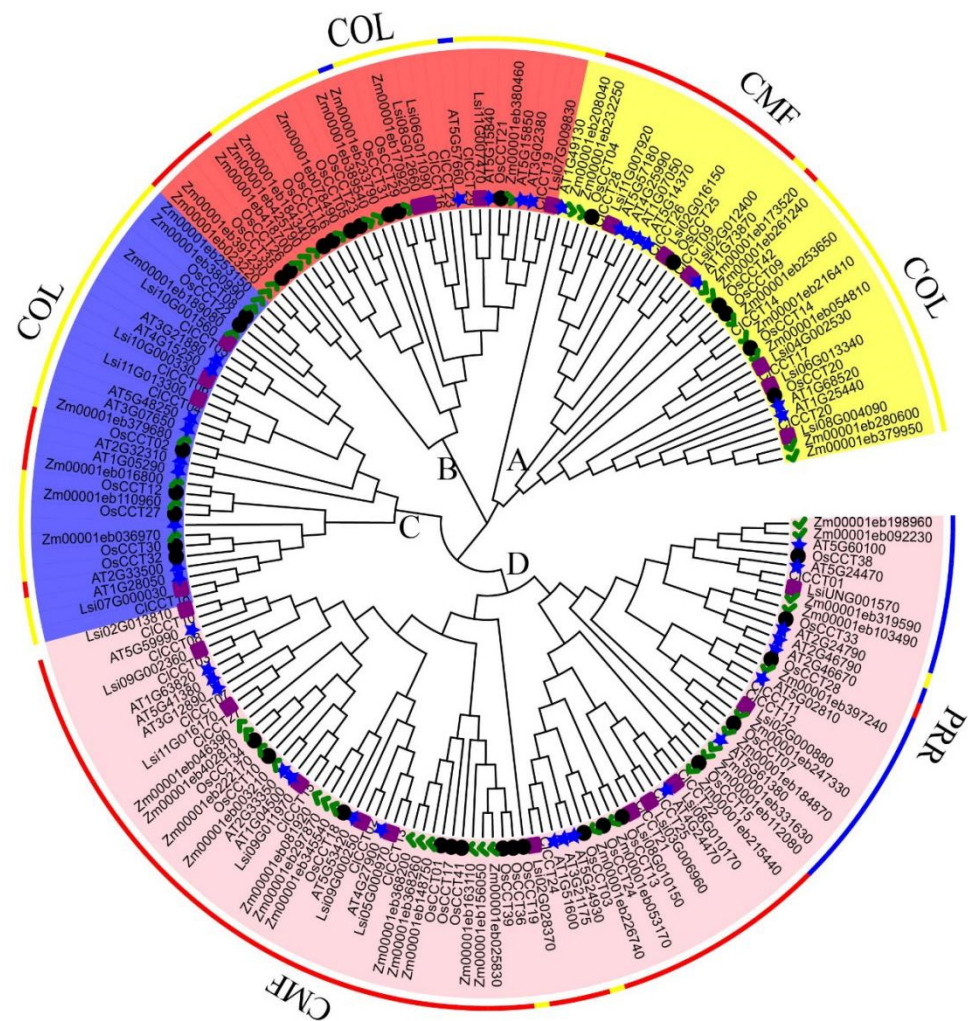


Figure 3. Phylogenetic relationships among CCT genes in *Citrullus lanatus*, *Arabidopsis*, bottle gourd, maize, and rice. The different colored circles indicate proteins of different subfamilies.

3.4. Cis-Acting Element Analyses of CICCT Genes

To more fully understand the processes that govern the expression of CICCT genes and their associated functions, 70 total predicted cis-acting elements were located within the 1.5 kb regions upstream of the translation start sites for these CICCT family members using the PlantCARE database. In addition to the common promoter cis-acting element, enhancer (CAAT-box) sequences, and core promoter elements, 17 additional cis-responsive elements were identified in these 29 CICCT genes (Table S5, Figure 4). Four of these cis-acting elements were related to light responsiveness, including the G-Box,

GT1-motif, Box 4, and TCT-motif elements. Additionally, eight stress-responsive elements were identified, including the ARE (anaerobic stress), W box (wounding), WUN-motif (wounding), WRE3 (wounding), O2-site (zein metabolism), LTR (cold), and MBS (drought) elements. Four hormone-responsive elements were identified, including the AAGAA-motif and ABRE sequences associated with ABA responses, as well as the TGACG-motif and CGTCA-motif related to MeJA responses. Of the analyzed CICCT genes, 90% were light-responsive. Following light-responsive elements, AREs were the most commonly detected cis-acting element among these watermelon genes, while MBS I elements were the least common. Figure 4 and Table S4, respectively, present the identification of these cis-acting elements and their predicted functions and positions. Together, these results suggest that CICCT family genes may be responsive to changing light levels, hormone production, and environmental conditions.

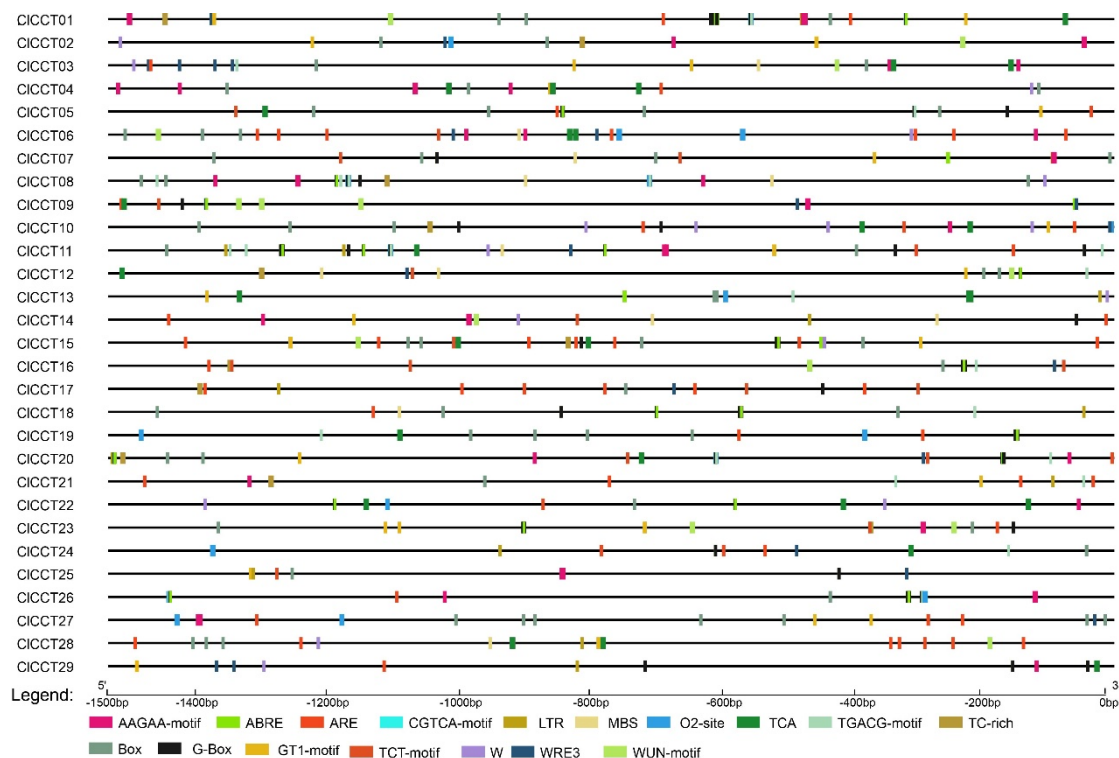


Figure 4. Cis-acting elements in CICCT promoters. The distribution of 14 cis-acting elements in the 1500 bp upstream promoter is shown. The different types of cis-acting elements are represented by different colors.

3.5. Characterization of CICCT Gene Responses to Multiple Stressors

Cis-acting element analyses of the promoters upstream of these CICCT genes suggested their potential involvement in stress responses (Figure 4), and these genes have also been reported to play various roles in resistance-related processes. As such, CICCT gene expression patterns in response to various stressors were next examined. Following exposure to cold stress, most of these genes did not exhibit any changes in expression (Figure 5). However, *CICCT17* expression was significantly reduced following 6 °C treatment for 24 h. *CICCT2*, *CICCT20*, and *CICCT28* were also slightly downregulated in response to cold stress, while *CICCT4* was slightly upregulated after being exposed to cold for 24 h. With the exception of *CICCT16*, these genes tended to be expressed at relatively low levels under cold stress and control conditions. The expression levels of subfamily III members were not significantly altered, remaining at relatively low levels of expression (Figure 5). Certain CICCT family members also exhibited responsivity to simulated drought stress. In general,

the expression of genes in subfamilies I, II, and III tended to remain relatively limited at baseline, with little change after drought induction (Figure 6). In contrast, subfamily IV genes were expressed at relatively high levels both before and after induction. While *CICCT11*, *CICCT17*, and *CICCT23* were expressed at relatively high levels, inconsistencies were observed among biological replicates, precluding further comparisons of these genes. In addition, *CICCT28* was significantly upregulated following drought induction for 8 days relative to control plants. Following exposure to salt stress for 7 h, *CICCT11*, *CICCT23*, as well as *CICCT04* and *CICCT28*, which are members of subfamilies I and II, were significantly reduced (Figure 7). In contrast, the expression levels of members of subfamilies III, IV, and V were not significantly responsive to salt stress (Figure 7).

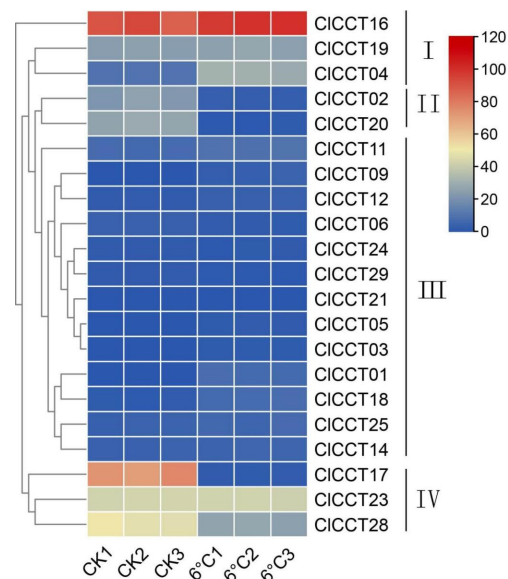


Figure 5. Expression levels analysis of CCT family in watermelon under 6 °C stress in watermelon (tissue: Leaf). Subdivided into groups (labeled I–IV) based on the transcriptome data. Blue genes indicate downregulated expression, while red genes indicate upregulated expression.

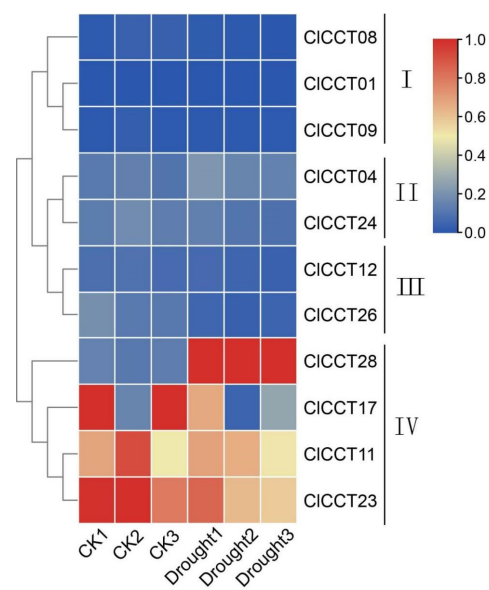


Figure 6. Expression levels analysis of CCT family in watermelon under drought stress in watermelon (Cultivar Crimson Sweet; tissue: Leaf; GEO: GSE144814). Subdivided into groups (labeled I–IV) based on the transcriptome data. Blue genes indicate downregulated expression, while red genes indicate upregulated expression.

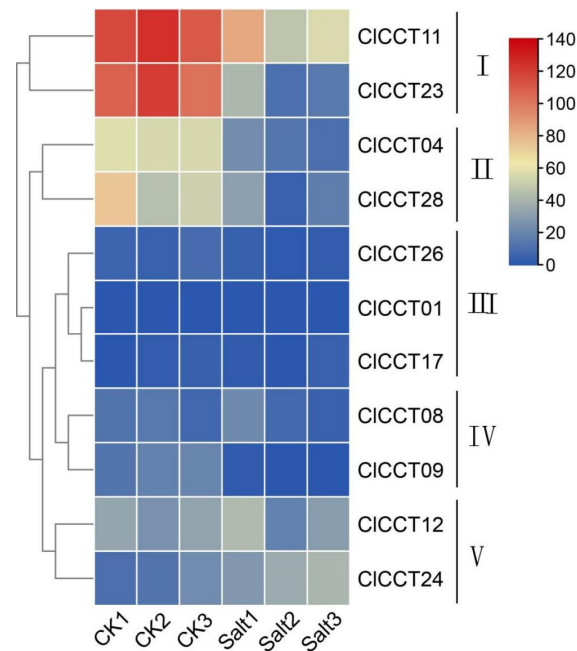


Figure 7. Expression levels analysis of CCT family in watermelon under salt stress in watermelon (Cultivar Crimson Sweet; tissue: Leaf; GEO: GSE146087). Subdivided into groups (labeled I–V) based on the transcriptome data. Blue genes indicate downregulated expression, while red genes indicate upregulated expression.

3.6. Evaluation of *CICCT* Gene Responsivity to Hormone Signaling

In many studies, CCT family genes have been shown to play key roles in various hormone signaling pathways. Here, the promoters of many *CICCT* genes were found to harbor hormone-responsive cis-acting elements, with the ABA-responsive AAGAA motif and ABREs being particularly common, along with the MeJA response-related CGTCA and TGACG motifs (Figure 4). In light of these observations, *CICCT* gene responses to treatment with ABA and MeJA were assessed via qPCR. The expression of all 29 of these genes was observed in response to ABA stress conditions after 0, 2, and 12 h. While some of these genes were upregulated significantly after 2 h (*CICCT2*, *CICCT13*, *CICCT19*), the downregulation of *CICCT2* and *CICCT19* was evident at 12 h (Figure 8). This suggests that these genes initially exhibit an upward expression trend followed by a downward trend. Only *CICCT13* expression levels rose continuously following ABA treatment for 12 h, peaking at levels four times higher than baseline. Conversely, the 6.7-fold inhibition of *CICCT7* expression was observed after ABA treatment for 2 h. After 12 h, this gene was expressed at slightly higher levels while remaining expressed at about ¼ of the control conditions. No significant differences in *CICCT17* or *CICCT20* expression were evident after ABA treatment for 2 h, whereas they were downregulated 12.5- and 2.5-fold, respectively, relative to control plants at 12 h (Figure 8). The relative expression of other members of this gene family was not altered significantly by hormone treatment, with their levels of relative expression remaining less than 2-fold different from those of controls. Following MeJA treatment for 2 h, no *CICCT* genes were significantly upregulated. After MeJA treatment for 12 h, *CICCT1*, *CICCT4*, *CICCT8*, *CICCT9*, *CICCT10*, *CICCT12*, and *CICCT29* were significantly upregulated, with an 8-fold increase being evident for *CICCT8*. *CICCT9*, *CICCT10*, *CICCT12*, and *CICCT29* were initially downregulated before subsequently being upregulated after MeJA treatment for 2 h (Figure 9). Conversely, *CICCT13*, *CICCT17*, *CICCT20*, and *CICCT28* expression was significantly suppressed following MeJA exposure for 2 h, with this suppression remaining evident after 12 h, including an 18-fold reduction in *CICCT17* levels relative to baseline. *CICCT14* and *CICCT26* expression was significantly

suppressed following MeJA treatment, whereas these expression levels recovered after 12 h. Other genes, such as *CICCT2*, *CICCT3*, *CICCT7*, *CICCT16*, and *CICCT19*, in contrast, were unaffected by MeJA (Figure 9).

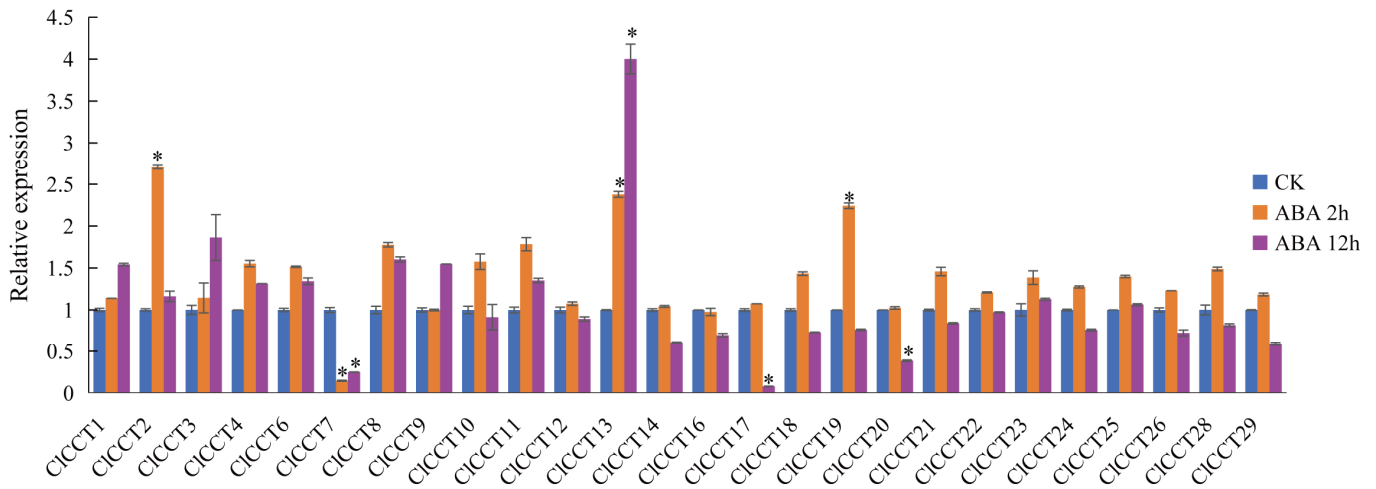


Figure 8. Expression analysis of *CICCT* genes under treatment of ABA hormones. The significant differences between data were calculated using Student's *t* test and indicated with an asterisk (*), $p < 0.05$.

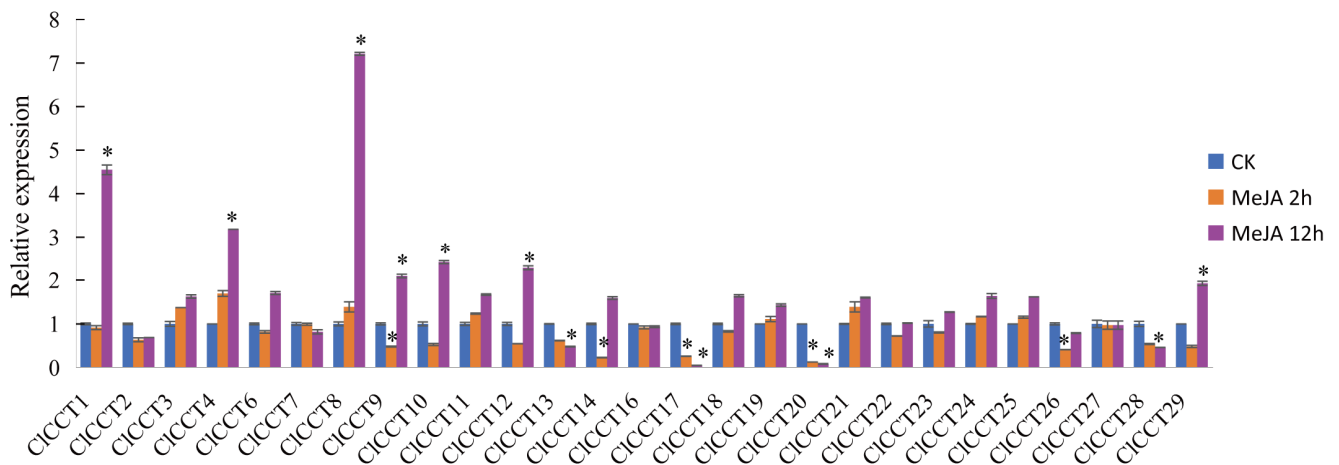


Figure 9. Expression analysis of *CICCT* genes under treatment of MeJA hormones. The significant differences between data were calculated using Student's *t* test and indicated with an asterisk (*), $p < 0.05$.

3.7. Analyses of *CICCT* Gene Responses to Photoperiod Prolongation

Certain CCT genes can regulate the timing of plant flowering. As many of the CCT genes identified in this study harbored cis-acting elements associated with photoresponsivity and diurnal rhythms, their potential control over the timing of plant flowering was explored by assessing their expression during the three-leaf stage under differing light conditions. In total, the expression of 24 of 29 *CICCT* genes was examined under conditions of photoperiod prolongation. As shown in Figure 10, a majority of these CCT genes were responsive to photoperiod. The downregulation of *CICCT3*, *CICCT7*, *CICCT18*, *CICCT21*, *CICCT22*, *CICCT25*, *CICCT28*, and *CICCT29* was observed during the day, whereas they were upregulated at night, with peak expression at 4 h into the night cycle. Of these genes, *CICCT3*, *CICCT7*, *CICCT21*, *CICCT22*, *CICCT25*, and *CICCT28* are CMF subfamily members, whereas *CICCT18* and *CICCT29* are COL subfamily members. Peak *CICCT2*, *CICCT4*, *CICCT6*, *CICCT9*, *CICCT10*, and *CICCT12* expression was evident during the night-to-day transition, whereas their expression was inhibited during the daytime before recovering at night. *CICCT4* and *CICCT6* are COL subfamily members, whereas *CICCT2*, *CICCT9*,

and *CICCT10* are CMF subfamily members. Peak *CICCT1*, *CICCT8*, *CICCT11*, *CICCT13*, *CICCT19*, and *CICCT23* expression was evident at 8 h into the day cycle. *CICCT16*, *CICCT17*, and *CICCT20*, which are COL subfamily genes, reached peak levels of expression at 4 h into the day cycle, whereas the lowest levels of *CICCT17* expression were evident at 8 h, and *CICCT16* and *CICCT20* levels fell to their lowest point at 12 h into the day cycle (Figure 10).

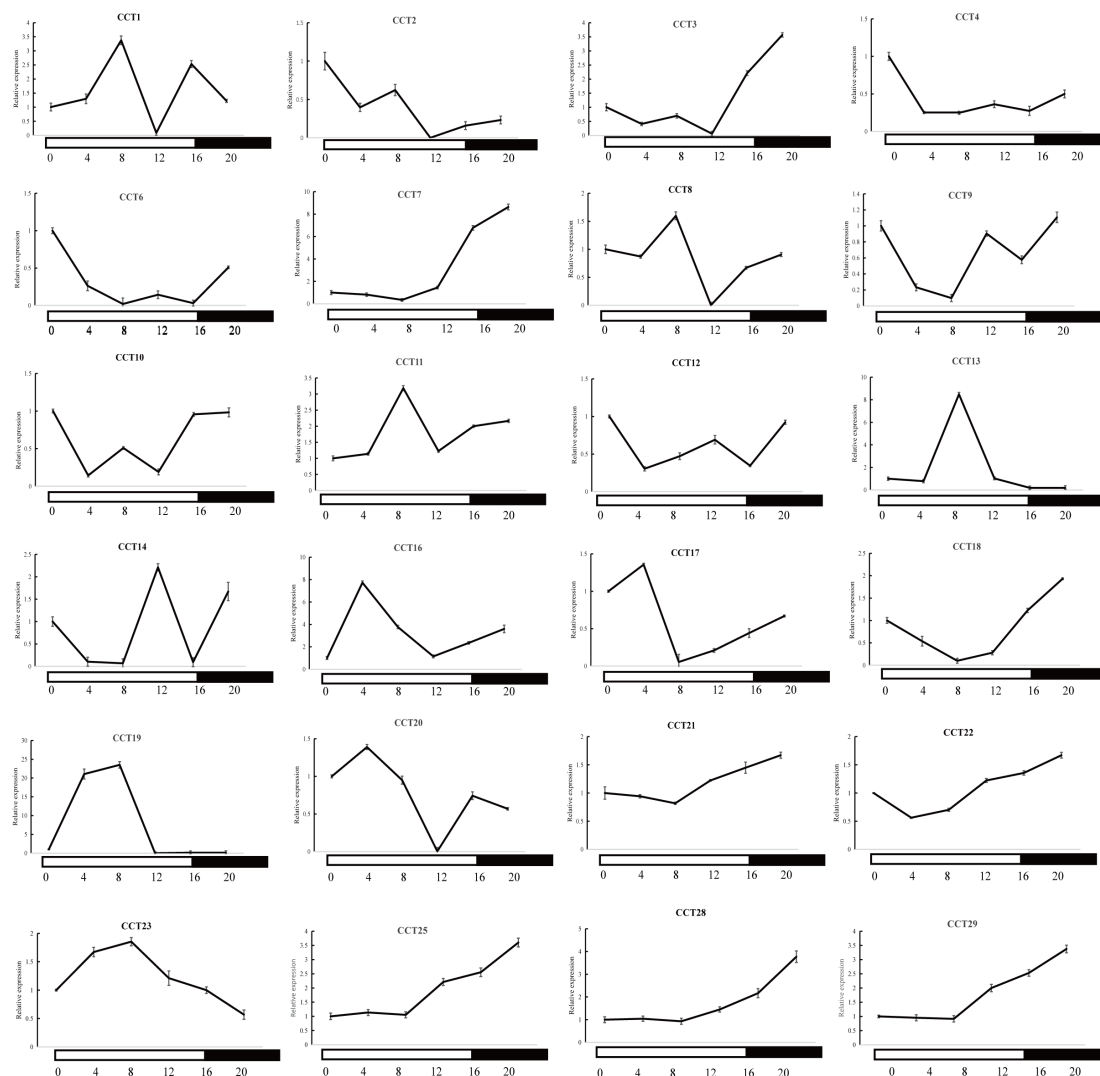


Figure 10. Expression pattern of *CICCT* genes under long days condition. White and black bars represent light and dark periods, respectively.

4. Discussion

Watermelon (*Citrullus lanatus*. L.) is an economically important member of the Cucurbitaceae family. Throughout the growth process, watermelon plants are often subjected to abiotic stressors, with the flowering period being a particularly important stage of development. Genes in the CCT family are involved in the regulation of both flowering and abiotic stress responses, comprising a key family of transcription factors. Here, 29 watermelon CCT family genes were identified. These genes exhibited isoelectric points from 4.02 to 10.13, and 24.1% were found to be alkaline (Table 1). Subcellular localization analyses suggested the nuclear localization of 75.9% of these CCT family members, while the next largest proportion was localized to chloroplasts, and just two exhibited predicted cytosolic localization. Members of the CCT family may thus play distinct roles in different compartments within cells (Table 1). This aligns well with prior reports pertaining to

OsCCT, SiCCT, AetCCT, MtCCT, TaCCT, and PtrCCT family genes [2,32–36]. The numbers of these watermelon CCT genes within the three established subfamilies were in line with those observed for *Arabidopsis*, bottle gourd, maize (Table S2) OsCCT genes [2], and similar characteristics were observed for SiCCT, AetCCT, MtCCT, TaCCT, and PtrCCT genes [32–36], with the CMF subfamily being the largest, followed by the COL and PRR subfamilies (Figures 3 and S7) [2,32–36].

The functional differentiation of members of multi-gene families is commonly observed over the course of evolution, including the loss or acquisition of specific conserved domains [37]. Genes in the COL and CMF subfamilies may have been absent or lost during the evolutionary or domestication processes [38]. The motifs, structural features, and genetic architecture of these genes may be central to the functional differences among members of these subfamilies (Figure 2), offering insight into the functional variability that exists among gene subfamilies and the ability of plants to adapt to shifting environmental conditions [39].

The three primary mechanisms that underlie gene family expansion include tandem duplication, segmental duplication, and transposition [40]. Protein-coding gene duplication events may lead to the loss or retention of the original functions of these genes or the emergence of novel functions [41]. During evolution, the replication of watermelon CCT genes was observed in various chromosomes. As shown in Figure 2, for instance, replication events were evident for *CICCT02/CICCT13*, *CICCT08/CICCT10*, *CICCT14/CICCT17*, *CICCT14/CICCT20*, and *CICCT07/CICCT27* (Figure 1). These five pairs of duplicated genes are all members of the same subfamily and are strongly evolutionarily related to one another, in addition to exhibiting structural similarities. The K_a/K_s values for all of these segmented repeat gene pairs were less than 1, indicating that net selection was the primary process affecting these *CICCT* genes (Table S3). These gene replication events have thus been subject to strong purifying selection during evolution, emphasizing the strong impact that these constraints can have on the emergence of replication events. In line with the CCT genes of other species, fragmental duplication events were most often observed, suggesting that these events are important for CCT gene family development [2,37–40]. Collinearity analyses of the CCT genes of watermelon and other species revealed the highest homology between the watermelon and gourd gene families. *CICCT15* homologs were detected in *Arabidopsis*, maize, and *Cucurbita*, indicating a potentially key role for this gene in the growth and evolution of plants. Linear relationships were observed for 27 CCT genes between *Citrullus lanatus* and *Lsiceraria* (dicot) (Table S4 and Figure S2), as well as 33 between *O. sativa* (monocot) and *Zea mays* L. (monocot) (Table S4 and Figure S4), suggesting that the CCT gene family members in *Citrullus lanatus* and *Lsiceraria*, *O. sativa* (monocot), and *Zea mays* L. are closely related. Linear relationships were observed for 2 CCT genes between *C. lanatus* and *Zea mays* L., as well as no gene between *C. lanatus* (dicot) and *O. sativa* (monocot) (Table S4 and Figure S3). Together, these results offer insights that can help guide future studies of CCT family gene functions.

Members of the CCT gene family play an essential role in the control of flowering, plant growth, grain yields, and stress responses [1]. Analyses of the cis-acting elements present in the promoters of CCT family genes suggested their potential responsiveness to phytohormones, light, and environmental stressors (Figure 4, Table S5). Here, significant changes in *CICCT17*, *CICCT2*, *CICCT20*, *CICCT28*, *CICCT4*, and *CICCT16* expression were observed in response to cold treatment (Figure 5). Cold-responsive elements were identified in the promoters of *CICCT17* and *CICCT28* (LTR; Figure 4), and these genes were downregulated following cold exposure, with the changes being more pronounced than those observed in other genes (Figure 5). When exposed to ABA, significant expression changes were observed in *CICCT2*, *CICCT13*, *CICCT19*, *CICCT7*, *CICCT17*, and *CICCT20*.

Except for *CICCT2*, all these genes contained ABA-responsive elements (ABRE) within their promoters (Figure 4). Exposure to MeJA stress did not alter the expression levels of *CICCT2*, *CICCT3*, *CICCT7*, *CICCT16*, and *CICCT19*, while other genes showed varying response patterns, with distinct response profiles among different family members (Figure 9). Although cis-elements related to MeJA are present in the promoters of *CICCT13* and *CICCT19*, they are absent from those of other CCT genes that respond to MeJA. This suggests their potential roles in plant cold resistance, salt stress, and hormonal stress. The presence of cis-acting elements in the stress response patterns of certain *CICCT* genes does not fully reflect the corresponding expression regulation. Similar phenomena have been observed in other species. Overexpression of *SICCT6* has been demonstrated to enhance drought resistance in tomatoes through the enhancement of antioxidant enzyme activity and the activation of stress-related genes [42]. In *Arabidopsis*, the CCT gene *PRR7* can augment tolerance to freezing conditions [43]. The apple *MdBBX10* protein increases the salt and osmotic stress resistance of *Escherichia coli* cells and participates in ROS and ABA-mediated responses [44].

Low-temperature stress can damage plant cells, reduce chlorophyll levels, and decrease photosynthetic activity [45,46]. Salt stress impairs plant cell membrane permeability and induces stomatal closure [47,48]. Drought stress leads to shortened meristematic tissues and disrupts cell cycle mechanisms in plants [49,50]. *CICCT17*, *CICCT4*, and *CICCT28*, members of the COL family, contain the B-box domain. The cysteine residues in this domain are essential for the protein's stress tolerance [44]. *CICCT04*'s expression levels significantly changed in response to low temperature and salt (Figures 5 and 7), and the gene also responded to MeJA (Figure 9). In *Arabidopsis thaliana*, *At5g48250* (*BBX8*) is closely related to *CICCT4* (Figure 3). In previous reports, the CRYPTOCHROME2 (CRY2)-COP1-HY5-BBX7/8 module has been demonstrated to regulate the blue light-dependent cold acclimation of *Arabidopsis* [51]. Additionally, *CICCT17* was sensitive to changing temperatures and was downregulated by 18-fold after MeJA treatment for 12 h (Figures 5 and 9). Previously, *MdBBX37*, a member of the COL family, has been shown to regulate cold stress resistance in apples, mediated by the plant hormone MeJA [52]. The expression pattern of *CICCT17* was the exact opposite, indicating that *CICCT17* may regulate watermelon's sensitivity to low temperature through the MeJA pathway. While *CICCT28* was responsive to low temperature, salt, and drought stresses, it did not respond to ABA treatment (Figures 5–8), indicating that the ABA signaling pathway may not play a role in controlling *CICCT28* expression in response to abiotic stressors. Research focused on the functional roles of *CICCT28* may, therefore offer value as a means of uncovering abiotic stress responses. Strikingly, *CICCT28* responds to MeJA treatment (Figure 9). These differing responses of CCT family genes to particular stressors may be indicative of the functional differentiation of members of this gene family. In addition, the same CCT genes may respond to abiotic stressors through a range of pathways, establishing a complex regulatory network.

A majority of plant CCT genes are related to the control of photoperiodic flowering, with their expression patterns being diurnal. In species such as *Arabidopsis* and rice, the gene and protein expression levels of PRR family members display a clear circadian rhythm [39,53,54]. The CCT motif of PRR is crucial for recognizing the circadian transcription factors CCA and LHY [39,53,54]. Members of the PRR family, including *AtPRR5/7/9* and *OsPRR37*, inhibit plant flowering under long-day conditions. These members are highly expressed in the morning, demonstrating a clear circadian rhythm at the transcriptional level [39,53,54]. *CICCT1* and *CICCT11*, which belong to the watermelon PRR subfamily, also exhibit significant circadian rhythms at the transcriptional level under long-day conditions, peaking in the morning. The gene *PRR5* (*AT5G24470*), which is closely related to *CICCT1*, is also a clock-related gene [55]. *CICCT1* and *CICCT11* may share similar functions

and mechanisms with *AtPRR5/7/9* and *OsPRR73*, and they also inhibit flowering under long-day conditions. *ZmCCT10* and *OsGhd7*, both members of the CMF subfamily, function as inhibitory factors in flowering responsive to photoperiod [14,56]. *ZmCCT10* delays the flowering phase of maize under long-day conditions by negatively modulating the maize flowering hormone gene *ZCN8* [56]. Conversely, *Ghd7* regulates *Ehd1*—a key factor in rice flowering, thereby controlling the expression of anthocyanin genes and inhibiting flowering under long-day conditions [14]. They both exhibit a diurnal rhythm with increased expression in the morning and decreased expression in the evening. Other members of the CMF subfamily, including *CICCT13*, *CICCT2*, and *CICCT8*, peak in the morning and also exhibit a similar diurnal rhythm under long-day conditions (Figure 10), suggesting that they may also inhibit flowering under these conditions. *OsCOL4* and *OsCOL10* also delay the flowering phase of rice under long-day conditions by negatively modulating *Ehd1*. *CICCT19* and *CICCT16*, two members of the COL subfamily, reach peak expression levels four hours into the day cycle, with expression levels 25 times or 8 times higher than the baseline, respectively (Figure 10). It is speculated that *CICCT19* and *CICCT16* may delay the flowering phase of watermelon under long-day conditions. The *CICCT25* homolog *At4g24470* (*GATA25*) of *CICCT25* exhibits circadian rhythmicity [57]. The *CICCT16* promoter region was found to harbor a cis-acting element involved in the regulation of circadian rhythms, consistent with similar reports for its closely related gene *At5g57660* (*COL5*) in *Arabidopsis* [58]. The overexpression of *AT1G25440* (*BBX15*), a gene closely related to *CICCT20* in *Arabidopsis* (Figure 7), results in late flowering [59]. These findings suggest that these genes may function similarly in watermelon. Genes in the CCT family control flowering and abiotic stress responses, highlighting the conservation of their functional roles across species. In addition, functional diversification was also evident for CCT family genes within species and among different members of this gene family.

Our research indicates that *CICCT17*, *CICCT28*, and *CICCT4* may respond to various abiotic stresses, presenting significant potential for watermelon breeding and genetic engineering. The functional study of these genes can be highly beneficial. Additionally, the transcription levels of most *CICCT* genes display rhythmicity under long-day conditions, suggesting a role in photoperiod regulation or circadian clock genes. This offers the possibility of developing early maturing or regionally adaptable watermelon varieties. Furthermore, certain CCT genes may delay watermelon flowering, and extending the growth period within a specific range could potentially result in larger fruits.

5. Conclusions

In this study, 29 watermelon CCT genes were identified and comprehensively analyzed based on their physicochemical characteristics, gene structures, chromosomal localization, cis-acting elements, and stressors. However, the role of cis-acting elements in stress responses and the diurnal expression patterns of certain *CICCT* genes do not fully reflect the corresponding expression regulation. Key insights, such as the identification of multifunctional genes like *CCT17*, *CICCT28*, and *CICCT4*, as well as the understanding of evolutionary relationships, are omitted. Our study provides valuable information and identifies candidate genes for crop improvement programs. In the future, we will focus on exploring how these genes may affect flowering and stress resilience under various environmental conditions.

Supplementary Materials: The following supporting information can be downloaded at: <https://www.mdpi.com/article/10.3390/agronomy15010232/s1>, Table S1. Primer sequences used for quantitative real-time PCR analysis. Table S2. Structures of the CCT proteins of *Arabidopsis*, bottle gourd and maize. Table S3. The Ka/Ks ratios and divergence between paralogous *CICCT* gene pairs. Table S4. CCTsynteny gene pairs between *A. thaliana* (dicot), *O. sativa* (monocot), *Zea mays*

L. (monocot) and *Lsiceraria* (dicot) genomes. Table S5. The *cis*-elements that have been identified in more than 9 CICCT genes. Figure S1. Distribution of *Citrullus lanatus* CCT genes on 11 chromosomes. Figure S2. Collinearity analysis of CICCT genes between *C. lanatus* and *A. thaliana/Lsiceraria*. Figure S3. Collinearity analysis of CICCT genes between *C. lanatus* and *O. sativa/Zea mays* L. Figure S4. Synteny analysis of CICCT genes between *O. sativa* and *A. thaliana/Zea mays* L. Figure S5. The CCT domains in the CICCT proteins. Figure S6. Ten types of conserved motifs in globe artichoke. Figure S7. The main conserved domain of CCT family genes in *Citrullus lanatus*.

Author Contributions: Conceptualization, Q.L. and M.L.; Methodology, N.X. and M.L.; Formal analysis, N.X. and Z.Z.; Writing original draft preparation, Y.H. and Q.L.; Writing review and editing, Q.L. and W.D.; Supervision, N.X., and M.L.; Funding acquisition, Q.L., J.S. and W.D.; Figures, Y.H. and Z.Z.; Resources and Data collection, J.S.; Literature search, Z.Z.; Study design, M.L. All authors have read and agreed to the published version of the manuscript.

Funding: This research was supported by Zhejiang Provincial Natural Science Foundation (Grant No. LY23C050001), Ningbo 2025 Key Technology Project of Yongjiang Science and Technology Innovation (Grant No. 2021Z132), the Youth Science and Technology Innovation Leading Talent Project of Ningbo, China (Grant No. 2024QL061), Natural Science Foundation of Ningbo City (Grant No. 2021J132); Ningbo 2035 Key Technology Project of Yongjiang Science and Technology Innovation (Grant No. 2024Z272).

Data Availability Statement: The raw data supporting the conclusions of this article will be made available by the authors on request.

Acknowledgments: We thank Kaixing Lu and Lili Chen for their help in the laboratory.

Conflicts of Interest: The authors declare no conflict of interest.

References

- Liu, H.; Zhou, X.; Li, Q.; Wang, L.; Xing, Y. CCT domain-containing genes in cereal crops: Flowering time and beyond. *Theor. Appl. Genet.* **2020**, *133*, 1385–1396. [[CrossRef](#)] [[PubMed](#)]
- Zhang, L.; Li, Q.; Dong, H.; He, Q.; Liang, L.; Tan, C.; Han, Z.; Yao, W.; Li, G.; Zhao, H.; et al. Three CCT domain-containing genes were identified to regulate heading date by candidate gene-based association mapping and transformation in rice. *Sci. Rep.* **2015**, *5*, 7663. [[CrossRef](#)] [[PubMed](#)]
- Robson, F.; Costa, M.M.; Hepworth, S.R.; Vizir, I.; Piñeiro, M.; Reeves, P.H.; Putterill, J.; Coupland, G. Functional importance of conserved domains in the flowering-time gene CONSTANS demonstrated by analysis of mutant alleles and transgenic plants. *Plant J.* **2001**, *28*, 619–631. [[CrossRef](#)] [[PubMed](#)]
- Zhang, J.; Hu, Y.; Xu, L.H.; He, Q.; Fan, X.W.; Xing, Y.Z. The CCT domain-containing gene family has large impacts on heading date, regional adaptation, and grain yield in rice. *J. Integr. Agric.* **2017**, *16*, 2686–2697. [[CrossRef](#)]
- Wu, W.; Zheng, X.M.; Lu, G.; Zhong, Z.; Gao, H.; Chen, L.; Wu, C.; Wang, H.J.; Wang, Q.; Zhou, K.; et al. Association of functional nucleotide polymorphisms at DTH2 with the northward expansion of rice cultivation in Asia. *Proc. Natl. Acad. Sci. USA* **2013**, *110*, 2775–2780. [[CrossRef](#)]
- Tribhuvan, K.U.; Kaila, T.; Srivastava, H.; Das, A.; Kumar, K.; Durgesh, K.; Jooshi, R.; Singh, B.K.; Singh, N.K.; Gaikwad, K. Structural and functional analysis of CCT family genes in pigeonpea. *Mol. Biol. Rep.* **2022**, *49*, 217–226. [[CrossRef](#)]
- Pearce, S.; Shaw, L.M.; Lin, H.; Cotter, J.D.; Li, C.; Dubcovsky, J. Night-break experiments shed light on the photoperiod1-mediated flowering. *Plant Physiol.* **2017**, *174*, 1139–1150. [[CrossRef](#)]
- Murphy, R.L.; Morishige, D.T.; Brady, J.A.; Rooney, W.L.; Yang, S.; Klein, P.E.; Mullet, J.E. *Ghd7* (Ma6) Represses sorghum flowering in long days: *Ghd7* alleles enhance biomass accumulation and grain production. *Plant Genome* **2014**. [[CrossRef](#)]
- Turner, A.; Beales, J.; Faure, S.; Dunford, R.P.; Laurie, D.A. The pseudo-response regulator Ppd-H1 provides adaptation to photoperiod in barley. *Science* **2005**, *310*, 1031–1034. [[CrossRef](#)]
- Shaw, L.M.; Lyu, B.; Turner, R.; Li, C.; Chen, F.; Han, X.; Fu, D.; Dubcovsky, J. FLOWERING LOCUS T2 regulates spike development and fertility in temperate cereals. *J. Exp. Bot.* **2019**, *70*, 193–204. [[CrossRef](#)] [[PubMed](#)]
- Höft, N.; Dally, N.; Jung, C. Sequence variation in the bolting time regulator BTC1 changes the life cycle regime in sugar beet. *Plant Breed.* **2018**, *137*, 412–422. [[CrossRef](#)]
- Wu, F.; Price, B.W.; Haider, W.; Seufferheld, G.; Nelson, R.; Hanzawa, Y. Functional and evolutionary characterization of the CONSTANS gene family in short-day photoperiodic flowering in soybean. *PLoS ONE* **2014**, *9*, e85754. [[CrossRef](#)] [[PubMed](#)]

13. Yoo, S.K.; Chung, K.S.; Kim, J.; Lee, J.H.; Hong, S.M.; Yoo, S.J.; Yoo, S.Y.; Lee, J.S.; Ahn, J.H. CONSTANS activates SUPPRESSOR OF OVEREXPRESSION OF CONSTANS 1 through FLOWERING LOCUS T to promote flowering in *Arabidopsis*. *Plant Physiol.* **2005**, *139*, 770–778. [[CrossRef](#)] [[PubMed](#)]
14. Xue, W.; Xing, Y.; Weng, X.; Zhao, Y.; Tang, W.; Wang, L.; Zhou, H.; Yu, S.; Xu, C.; Li, X.; et al. Natural variation in *Ghd7* is an important regulator of heading date and yield potential in rice. *Nat. Genet.* **2008**, *40*, 761–767. [[CrossRef](#)] [[PubMed](#)]
15. Yan, W.H.; Wang, P.; Chen, H.X.; Zhou, H.J.; Li, Q.P.; Wang, C.R.; Ding, Z.H.; Zhang, Y.S.; Yu, S.B.; Xing, Y.Z.; et al. A major *QTL*, *Ghd8*, plays pleiotropic roles in regulating grain productivity, plant height, and heading date in rice. *Mol. Plant* **2011**, *4*, 319–330. [[CrossRef](#)] [[PubMed](#)]
16. Yan, W.; Liu, H.; Zhou, X.; Li, Q.; Zhang, J.; Lu, L.; Liu, T.; Liu, H.; Zhang, C.; Zhang, Z.; et al. Natural variation in *Ghd7.1* plays an important role in grain yield and adaptation in rice. *Cell Res.* **2013**, *23*, 969–971. [[CrossRef](#)]
17. Kumar, V. CONSTANS regulates seed size in a photoperiod-dependent manner. *Plant Growth Regul.* **2024**, *104*, 77–80. [[CrossRef](#)]
18. Achary, R.K.; Majee, M. CONSTANS, a key-player connecting day length to seed size. *Trends Plant Sci.* **2023**, *28*, 975–977. [[CrossRef](#)]
19. Muhammad, I.; Shalmani, A.; Ali, M.; Yang, Q.H.; Ahmad, H.; Li, F.B. Mechanisms regulating the dynamics of photosynthesis under abiotic stresses. *Front. Plant Sci.* **2021**, *11*, 615942. [[CrossRef](#)] [[PubMed](#)]
20. Kurepin, L.V.; Ivanov, A.G.; Zaman, M.; Pharis, R.P.; Allakhverdiev, S.I.; Hurry, V.; Hüner, N.P. Stress-related hormones and glycinebetaine interplay in protection of photosynthesis under abiotic stress conditions. *Photosynth. Res.* **2015**, *126*, 221–235. [[CrossRef](#)]
21. Choudhary, P.; Aggarwal, P.R.; Salvi, P.; Muthamilarasan, M. Molecular insight into auxin signaling and associated network modulating stress responses in rice. *Plant Physiol. Biochem.* **2024**, *219*, 109452. [[CrossRef](#)]
22. Liu, J.; Shen, J.; Xu, Y.; Li, X.; Xiao, J.; Xiong, L. *Ghd2*, a CONSTANS-like gene, confers drought sensitivity through regulation of senescence in rice. *J. Exp. Bot.* **2016**, *67*, 5785–5798. [[CrossRef](#)] [[PubMed](#)]
23. Wei, H.; Wang, X.; He, Y.; Xu, H.; Wang, L. Clock component *OsPRR73* positively regulates rice salt tolerance by modulating *OsHKT2;1* mediated sodium homeostasis. *EMBO J.* **2020**, *40*, e105086. [[CrossRef](#)]
24. Min, J.H.; Chung, J.S.; Lee, K.H.; Kim, C.S. The CONSTANS-like 4 transcription factor, *AtCOL4*, positively regulates abiotic stress tolerance through an abscisic acid-dependent manner in *Arabidopsis*. *J. Integr. Plant Biol.* **2015**, *57*, 313–324. [[CrossRef](#)]
25. Su, H.; Liang, J.; Abou-Elwafa, S.; Cheng, H.; Dou, D.; Ren, Z.; Xie, J.; Chen, Z.; Gao, F.; Ku, L.; et al. *ZmCCT* regulates photoperiod-dependent flowering and response to stresses in maize. *BMC Plant Biol.* **2021**, *21*, 453. [[CrossRef](#)] [[PubMed](#)]
26. Wang, Y.; Wang, L.; Xing, N.; Wu, X.; Wu, X.; Wang, B.; Lu, Z.; Xu, P.; Tao, Y.; Li, G.; et al. A universal pipeline for mobile mRNA detection and insights into heterografting advantages under chilling stress. *Hortic. Res.* **2020**, *7*, 13. [[CrossRef](#)] [[PubMed](#)]
27. Song, Q.; Joshi, M.; Joshi, V. Transcriptomic analysis of short-term salt stress response in watermelon seedlings. *Int. J. Mol. Sci.* **2020**, *21*, 6036. [[CrossRef](#)]
28. Song, Q.; Joshi, M.; DiPiazza, J.; Joshi, V. Functional Relevance of Citrulline in the Vegetative Tissues of Watermelon During Abiotic Stresses. *Front. Plant Sci.* **2020**, *11*, 512. [[CrossRef](#)] [[PubMed](#)]
29. Wheeler, T.J.; Eddy, S.R. nhmmer: DNA homology search with profile HMMs. *Bioinformatics* **2013**, *29*, 2487–2489. [[CrossRef](#)] [[PubMed](#)]
30. Voorrips, R.E. MapChart: Software for the graphical presentation of linkage maps and QTLs. *J. Hered.* **2002**, *93*, 77–78. [[CrossRef](#)]
31. Koch, M.A.; Haubold, B.; Mitchell-Olds, T. Comparative evolutionary analysis of chalcone synthase and alcohol dehydrogenase loci in *Arabidopsis*, *Arabis*, and related genera (*Brassicaceae*). *Mol. Biol. Evol.* **2000**, *17*, 1483–1498. [[CrossRef](#)] [[PubMed](#)]
32. Li, Y.; Yu, S.; Zhang, Q.; Wang, Z.; Liu, M.; Zhang, A.; Dong, X.; Fan, J.; Zhu, Y.; Ruan, Y.; et al. Genome-wide identification and characterization of the CCT gene family in foxtail millet (*Setaria italica*) response to diurnal rhythm and abiotic stress. *Genes* **2022**, *13*, 1829. [[CrossRef](#)]
33. Zheng, X.; Li, X.; Ge, C.; Chang, J.; Shi, M.; Chen, J.; Qiao, L.; Chang, Z.; Zheng, J.; Zhang, J. Characterization of the CCT family and analysis of gene expression in *Aegilops tauschii*. *PLoS ONE* **2017**, *12*, e0189333. [[CrossRef](#)]
34. Ma, L.; Yi, D.; Yang, J.; Liu, X.; Pang, Y. Genome-wide identification, expression analysis and functional study of CCT gene family in *Medicago truncatula*. *Plants* **2020**, *9*, 513. [[CrossRef](#)] [[PubMed](#)]
35. Zhang, H.; Jiao, B.; Dong, F.; Liang, X.; Zhou, S.; Wang, H. Genome-wide identification of CCT genes in wheat (*Triticum aestivum* L.) and their expression analysis during vernalization. *PLoS ONE* **2022**, *17*, e0262147. [[CrossRef](#)] [[PubMed](#)]
36. Chen, H.; Zhang, S.; Du, K.; Kang, X. Genome-wide identification, characterization, and expression analysis of CCT transcription factors in poplar. *Plant Physiol. Biochem.* **2023**, *204*, 108101. [[CrossRef](#)]
37. Omichinski, J.G.; Clore, G.M.; Schaad, O.; Felsenfeld, G.; Trainor, C.; Appella, E.; Stahl, S.J.; Gronenborn, A.M. NMR structure of a specific DNA complex of Zn-containing DNA binding domain of GATA-1. *Science* **1993**, *261*, 438–446. [[CrossRef](#)] [[PubMed](#)]
38. Cockram, J.; Thiel, T.; Steuernagel, B.; Stein, N.; Taudien, S.; Bailey, P.C.; O'Sullivan, D.M. Genome dynamics explain the evolution of flowering time CCT domain gene families in the Poaceae. *PLoS ONE* **2012**, *7*, e45307. [[CrossRef](#)]

39. Liu, C.; Qu, X.F.; Zhou, Y.H.; Song, G.Y.; Abiri, N.; Xiao, Y.H.; Liang, F.; Jiang, D.M.; Hu, Z.L.; Yang, D.C. *OsPRR37* confers an expanded regulation of the diurnal rhythms of the transcriptome and photoperiodic flowering pathways in rice. *Plant Cell Environ.* **2018**, *41*, 630–645. [[CrossRef](#)]
40. Kong, H.Z.; Landherr, L.L.; Frohlich, M.W.; Leebens-Mack, J.; Ma, H.; DePamphilis, C.W. Patterns of gene duplication in the plant *SKP1* gene family in angiosperms: Evidence for multiple mechanisms of rapid gene birth. *Plant J.* **2007**, *50*, 873–885. [[CrossRef](#)] [[PubMed](#)]
41. Hughes, T.; Liberles, D.A. The pattern of evolution of smaller-scale gene duplicates in mammalian genomes is more consistent with neo-than subfunctionalisation. *J. Mol. Evol.* **2007**, *65*, 574–588. [[CrossRef](#)] [[PubMed](#)]
42. Huang, S.; Yang, X.; Li, W.; Xu, Z.; Xie, Y.; Meng, X.; Li, Z.; Zhou, W.; Wang, S.; Jin, L. Genome-wide analysis of the CCT gene family and functional characterization of *SICCT6* in response to drought stress in tomato. *Int. J. Biol. Macromol.* **2024**, *280*, 135906. [[CrossRef](#)]
43. Kim, Y.J.; Kim, W.Y.; Somers, D.E. HOS15-mediated turnover of *PRR7* enhances freezing tolerance. *New Phytol.* **2024**, *244*, 798–810. [[CrossRef](#)] [[PubMed](#)]
44. Liu, X.; Dai, Y.Q.; Li, R.; Yuan, L.; Chen, X.S.; Wang, X.Y. Members of B-box protein family from *Malus domestica* enhanced abiotic stresses tolerance in *Escherichia coli*. *Mol. Biotechnol.* **2019**, *61*, 421–426. [[CrossRef](#)]
45. Mattila, H.; Mishra, K.B.; Kuusisto, I.; Mishra, A.; Novotná, K.; Šebela, D.; Tyystjärvi, E. Effects of low temperature on photoinhibition and singlet oxygen production in four natural accessions of *Arabidopsis*. *Planta* **2020**, *252*, 19. [[CrossRef](#)] [[PubMed](#)]
46. Lee, H.J.; Lee, J.H.; Wi, S.; Jang, Y.; An, S.; Choi, C.K.; Jang, S. Exogenously applied glutamic acid confers improved yield through increased photosynthesis efficiency and antioxidant defense system under chilling stress condition in *Solanum lycopersicum* L. cv. Dotaerang Dia. *Sci. Hort.* **2021**, *277*, 109817. [[CrossRef](#)]
47. Oliveira, A.B.; Alencar, N.L.; Gomes-Filho, E. ‘Comparison between the water and salt stress effects on plant growth and development’, responses of organisms to water stress. *InTech* **2013**, *4*, 67–94.
48. Garg, A.; Bordoloi, S.; Ganesan, S.P.; Sekharan, S.; Sahoo, L. A relook into plant wilting: Observational evidence based on unsaturated soil-plant-photosynthesis interaction. *Sci. Rep.* **2020**, *10*, 22064. [[CrossRef](#)] [[PubMed](#)]
49. Granier, C.; Inze, D.; Tardieu, F. Spatial distribution of cell division rate can be deduced from that of p34cdc2 kinase activity in maize leaves grown at contrasting temperatures and soil water conditions. *Plant Physiol.* **2000**, *124*, 1393–1402. [[CrossRef](#)] [[PubMed](#)]
50. Carneiro, A.K.; Montessoro, P.D.F.; Fusaro, A.F.; Araújo, B.G.; Hemerly, A.S. Plant CDKs-driving the cell cycle through climate change. *Plants* **2021**, *10*, 1804. [[CrossRef](#)] [[PubMed](#)]
51. Li, Y.; Shi, Y.; Li, M.; Fu, D.; Wu, S.; Li, J.; Gong, Z.; Liu, H.; Yang, S. The CRY2-COP1-HY5-BBX7/8 module regulates blue light-dependent cold acclimation in *Arabidopsis*. *Plant Cell* **2021**, *33*, 3555–3573. [[CrossRef](#)] [[PubMed](#)]
52. An, J.P.; Wang, X.F.; Zhang, X.W.; You, C.X.; Hao, Y.J. Apple B-box protein BBX37 regulates jasmonic acid mediated cold tolerance through the JAZ-BBX37-ICE1-CBF pathway and undergoes MIEL1-mediated ubiquitination and degradation. *New Phytol.* **2021**, *229*, 2707–2729. [[CrossRef](#)]
53. Matsushika, A.; Makino, S.; Kojima, M.; Mizuno, T. Circadian waves of expression of the APRR1/TOC1 family of pseudo-response regulators in *Arabidopsis thaliana*: Insight into the plant circadian clock. *Plant Cell Physiol.* **2000**, *41*, 1002–1012. [[CrossRef](#)]
54. Yang, N.; Wang, Y.B.; Liu, X.G.; Jin, M.L.; Vallebuena-Estrada, M.; Calfee, E.; Chen, L.; Dilkes, B.P.; Gui, S.T.; Fan, X.M.; et al. Two teosintes made modern maize. *Science* **2023**, *382*, eadg8940. [[CrossRef](#)] [[PubMed](#)]
55. De Los Reyes, P.; Serrano-Bueno, G.; Romero-Campero, F.J.; Gao, H.; Romero, J.M.; Valverde, F. CONSTANS alters the circadian clock in *Arabidopsis thaliana*. *Molecular Plant* **2024**, *17*, 1204–1220. [[CrossRef](#)]
56. Zhao, Y.; Zhao, B.; Xie, Y.; Jia, H.; Li, Y.; Xu, M.; Wu, G.; Ma, X.; Li, Q.; Hou, M.; et al. The evening complex promotes maize flowering and adaptation to temperate regions. *Plant Cell* **2023**, *35*, 369–389. [[CrossRef](#)]
57. Manfield, I.W.; Devlin, P.F.; Jen, C.H.; Westhead, D.R.; Gilmartin, P.M. Conservation, convergence, and divergence of light-responsive, circadian-regulated, and tissue-specific expression patterns during evolution of the *Arabidopsis* GATA gene family. *Plant Physiol.* **2007**, *143*, 941–958. [[CrossRef](#)] [[PubMed](#)]
58. Hassidim, M.; Harir, Y.; Yakir, E.; Kron, I.; Green, R.M. Over-expression of CONSTANS-LIKE 5 can induce flowering in short-day grown *Arabidopsis*. *Planta* **2009**, *230*, 481–491. [[CrossRef](#)] [[PubMed](#)]
59. Susila, H.; Nasim, Z.; Gawarecka, K.; Jung, J.Y.; Jin, S.; Youn, G.; Ahn, J.H. Chloroplasts prevent precocious flowering through a GOLDEN2-LIKE-B-BOX DOMAIN PROTEIN module. *Plant Commun.* **2023**, *4*, 100515. [[CrossRef](#)] [[PubMed](#)]

Disclaimer/Publisher’s Note: The statements, opinions and data contained in all publications are solely those of the individual author(s) and contributor(s) and not of MDPI and/or the editor(s). MDPI and/or the editor(s) disclaim responsibility for any injury to people or property resulting from any ideas, methods, instructions or products referred to in the content.